Vol. 598: 35–48, 2018
https://doi.org/10.3354/meps12612

MARINE ECOLOGY PROGRESS SERIES
Mar Ecol Prog Ser

Published June 28

Fine-scale depth structure of pelagic communities throughout the global ocean based on acoustic sound scattering layers

Roland Proud[1,*], Martin J. Cox[2], Camille Le Guen[1], Andrew S. Brierley[1]

[1]Pelagic Ecology Research Group, Scottish Oceans Institute, Gatty Marine Laboratory, School of Biology, University of St Andrews KY16 8LB, UK

[2]Australian Antarctic Division, Kingston, Tasmania 7050, Australia

ABSTRACT : Most multicellular biomass in the mesopelagic zone (200–1000 m) comprises zooplankton and fish aggregated in layers known as sound scattering layers (SSLs), which scatter sound and are detectable using echosounders. Some of these animals migrate vertically to and from the near surface on a daily cycle (diel vertical migration, DVM), transporting carbon between the surface and the deep ocean (biological carbon pump, BCP). To gain insight into potential global variability in the contribution of SSLs to the BCP, and to pelagic ecology generally (SSLs are likely prey fields for numerous predators), we investigated regional-scale (90 000 km^2) community depth structure based on the fine-scale (10s of m) vertical distribution of SSLs. We extracted SSLs from a near-global dataset of 38 kHz echosounder observations and constructed local (300 km × 300 km) SSL depth and echo intensity (a proxy for biomass) probability distributions. The probability distributions fell into 6 spatially coherent regional-scale SSL probability distribution (RSPD) groups. All but 1 RSPD exhibited clear DVM, and all RSPDs included stable night-time resident deep scattering layers (DSLs: SSLs deeper than 200 m). Analysis of DSL number and stability (probability of observation at depth) revealed 2 distinct DSL types: (1) single-shallow DSL (a single DSL at ca. 500 m) and (2) double-deep DSL (2 DSLs at ca. 600 and 850 m). By including consideration of this fine-scale depth structure in biogeographic partitions and ecosystem models, we will better understand the role of mesopelagic communities in pelagic food webs and the consequences of climate change for these communities.

KEY WORDS: Biogeography · Diel vertical migration · DVM · Acoustics · Water column · Deep scattering layer · DSL · Mesopelagic

INTRODUCTION

The biological carbon pump (BCP), which is in part mediated by the regular vertical migrations of mesopelagic organisms, transfers large quantities of carbon from the atmosphere to the deep ocean (Anderson et al. 2018). The atmospheric concentration of carbon dioxide is presently estimated to be about 200 ppm lower than it would otherwise be in the absence of the BCP (Parekh et al. 2006). Using scientific echosounders, the diel vertical migration (DVM) that is integral to the operation of the BCP can be detected as the upward and downward migrations at dusk and dawn of the open-ocean communities that comprise acoustic deep scattering layers (DSLs; sound scattering layers deeper than 200 m). The fine-scale (10s of m) depth structure of these communities will likely impact the efficiency of the BCP (see Klevjer et al. 2016) and the foraging behaviour of air-breathing deep-diving predators including northern and southern elephant seals *Mirounga* spp. and king penguins *Aptenodytes patagonicus* (Scheffer et al.

*Corresponding author: rp43@st-andrews.ac.uk

2010, Boersch-Supan et al. 2012). It is therefore important to consider regional variability in open-ocean community depth structure in studies of open-ocean ecology and in the design of open-ocean ecosystem/biogeochemical models such as SEAPODYM, Atlantis and MIZER (Lehodey et al. 2008, Fulton et al. 2011, Trebilco et al. 2013, Scott et al. 2014), which are in turn important components of climate models (Giering et al. 2014). Variability in depth structure should also be considered when partitioning the global ocean into ecological regions (Proud et al. 2017, Sutton et al. 2017).

Vertical structure of water-column communities

From the sea surface to 1000 m deep, the pelagic zone (i.e. the water column away from the seabed) can be divided into 2 zones, the epipelagic (0 to 200 m) and the mesopelagic (200 to 1000 m). The epipelagic contains an illuminated mixed layer that is isothermal and usually bounded by a steep seasonal thermocline, which is variable in depth. The epipelagic is the site of oceanic primary production (PP), the magnitude of which is a function of light intensity, temperature and nutrient availability (via mixing). PP varies widely both geographically and over time (Boyce et al. 2010, 2012), and PP variability has been a prominent basis for partitioning the global ocean into ecological regions, such as the 'provinces' derived by Longhurst (2007). The mesopelagic is typically colder than the epipelagic, and seawater there is denser. Key inhabitants of the mesopelagic are the zooplankton, squid and small bony fishes that aggregate in layers and which generally migrate daily (i.e. undertake DVM) upwards towards the surface at dusk to feed before returning to depth at dawn (Bianchi et al. 2013, Bianchi & Mislan 2016). However, not all organisms migrate daily, and 'resident' night-time mesopelagic communities have often been observed (Koslow et al. 1997, Flynn & Kloser 2012). Generally, the migrating community follows low-light intensity isolumes, such that they ascend to feed whilst minimising the risk of being detected by visual predators (Hays 2003). Daily movements and rest periods at depth facilitate transport of carbon, nutrients and energy (via respiration and excretion) from the surface to deep water (Schnetzer & Steinberg 2002). Seasonal community movements, including overwintering at depth by copepods, also contribute to nutrient and energy flux (Jónasdóttir et al. 2015).

DSLs

DSLs, which form in the mesopelagic zone, take their name from the fact that they scatter sound. A consequence of this is that they can be detected using active acoustic sampling (scientific echosounding). The depth at which DSLs are located varies geographically and seasonally (Anderson et al. 2005, Kloser et al. 2009, Irigoien et al. 2014, Knutsen et al. 2017, Proud et al. 2017). This variability is thought to be predictable, since observed depths of DSLs have been linked to environmental drivers such as seawater density (Godø et al. 2012), light intensity (Hays 2003, Aksnes et al. 2017, Proud et al. 2017), oxygen concentration (Bianchi et al. 2013, Klevjer et al. 2016) and wind-driven mixing (Proud et al. 2017). Furthermore, regional variability in the intensity of echoes from DSLs, a rough proxy for biomass, has been linked to PP in the waters above and to temperature (Irigoien et al. 2014, Fennell & Rose 2015, Proud et al. 2017). There is often more than one DSL in a given location (Andreeva et al. 2000), and DSLs at different depths likely comprise different communities (the stacked DSLs can be considered as rungs in the 'ladders of migration' sensu Vinogradov 1968). The vertical distributions of these multiple DSLs can shift at twilight, with some migrating in unison, some remaining stationary, some merging, and some splitting, such that there are distinct day and night patterns (e.g. Klevjer et al. 2012). These complex and variable depth structures vary globally and may well be intimately linked to concomitant environmental variability. By characterising the form and variability of these depth structures, we inadvertently characterise complex and distinct environments, which may enable improved partitioning of the ocean into biogeographic regions.

Biogeography

Historically, biogeographic partitioning of the ocean was generally performed using just biological data (Brinton 1962, Alvarino 1965, Briggs 1974, Semina 1997), but more recent classifications have been able to capitalise on the availability of open-access data and to incorporate numerous data sources (including biological, chemical and physical) into their partitioning algorithms (Longhurst 2007, Proud et al. 2017, Sayre et al. 2017, Sutton et al. 2017). Distributions and abundances of species and 'environmental' parameters vary with depth, so it is not necessary to expect that the same spatial grid of clas-

sification at the surface, for example, would pertain to the mesopelagic. Further, the number of separate classes, units or provinces that can be identified/discriminated depends on many factors, including geographic scale and number of variables considered. In most cases, the number of separations can be considered to be an arbitrary, artificial construct, and is usually selected for a specific purpose, e.g. management (e.g. Sayre et al. 2017) or research applications. Biogeographies vary by depth strata, from surface and epipelagic classification (Longhurst 2007, Oliver & Irwin 2008, Spalding et al. 2012), mesopelagic and water-column (Flynn & Marshall 2013, Proud et al. 2017, Sayre et al. 2017, Sutton et al. 2017) to seabed (UNESCO 2009, Watling et al. 2013). However, none have included detailed (10s of m) water-column community depth structure because data have not been readily available.

Hypothesis and objectives

The biophysical drivers of DSL depth and echo intensity (a proxy for biomass; Proud et al. 2018) have been used to demark global biogeographies (Proud et al. 2017). We therefore hypothesised that distinct communities, with distinct depth preferences, exist and that these preferences lead to spatially coherent vertical structuring at regional scales. To test this hypothesis, our approach was as follows: (1) extract sound scattering layer (SSL; non-depth-specific scattering layer) depth, thickness and echo intensity (between 0 and 1200 m) from globally collated 38 kHz echosounder data using the SSL extraction method (SSLEM, Proud et al. 2015); (2) produce local (300 km × 300 km) SSL probability distributions (SPDs), which provide, for a given area, the probability of observing an SSL at a specific depth and echo intensity value; (3) cluster the SPDs by likeness and derive regional-scale SPDs (RSPDs) and (4) categorise RSPDs by DSL depth structure and vertical stability, defined as the probability of DSL observation at its principal, or most common, depth (e.g. where a DSL is always observed at a certain depth for a specific RSPD, DSL vertical stability would equal 1).

METHODS

SSLs were extracted from an extensive acoustic dataset (38 kHz echograms, n = 3196, equal to 380 days of observations), spatially binned into 300 km × 300 km cells (90 000 km^2), grouped by day and night, and summarised by depth and mean volume backscattering strength (MVBS, dB re 1 m^{-1}, Maclennan et al. 2002) SPDs. SSLs that had a mean depth >200 m were defined as DSLs. Cluster analysis was used to group similar SPDs in space, and RSPDs were defined, enabling inferences on the underlying biological communities to be made.

Acoustic data

Echosounder observations (38 kHz), recorded between 2006 and 2015, were collated from the British Oceanographic Data Centre (BODC, www.bodc.ac.uk), the British Antarctic Survey (BAS 2015), the Pelagic Ecology Research Group (PERG, www.risweb.st-andrews.ac.uk/portal/en/) and the Integrated Marine Observing System (IMOS, www.imos.org.au). Seasonal coverage was variable, ranging from near uniform sampling with full seasonal coverage in the South Indian Ocean, to regions with lower sampling coverage (1–2 seasons) in the polar and North Pacific regions (polar regions are not typically sampled during winter due to sea ice cover).

Data were calibrated and noise was removed (see the supplemental information in Proud et al. 2017 for details of data processing). SSLs persisting for longer than 30 min were extracted and characterised using the SSLEM (Proud et al. 2015). Individual SSLs were described by their mean depth, thickness and MVBS, and binned by geographic location onto a uniform global 300 km × 300 km grid (where seabed depth >1000 m) as per the spatial scale applied by Proud et al. (2017). Gridded SSLs were grouped by day and night periods (demarked using local sunrise and sunset times) and summarised by depth and MVBS SPDs.

SPDs

Following Proud et al. (2017), we defined the probability (P) of observing an SSL at a specific depth (z) and MVBS value as:

$$P_{z,MVBS} = \frac{obs_{z,MVBS}}{se_z} \quad (1)$$

where $obs_{z,MVBS}$ is the total time of SSL observation (s) by depth (0 to 1200 m by 5 m intervals) and MVBS level (–50 to –100 dB re 1 m^{-1}, by 2 dB re 1 m^{-1} intervals) and se_z is the sampling effort (s) by depth, i.e. for each depth interval, the probability of SSL observation (including the probability of no observation) sums to 1. Calculating P over the entire depth and

MVBS range yielded an SPD for each geographic cell for both day and night.

Seasonal coverage index (SCI)

To quantify the temporal distribution of echosounder observations for each SPD, we calculated a seasonal coverage index (SCI), given by:

$$\mathrm{SCI} = \sum_{i=1}^{4} \mathrm{se}_i \,/\, max(\mathrm{se}_1, \mathrm{se}_2, \mathrm{se}_3, \mathrm{se}_4) \quad (2)$$

where se_i is the sampling effort (s) for each season, represented by the integer i, ranging from 1 (spring) to 4 (winter), and *max* is a function that returns the maximum value of a given vector. For an SPD where all observations were made in a single season, SCI would equal 1, whereas for an SPD where the sampling effort for all 4 seasons was the same (uniform distribution), SCI would equal 4.

Epipelagic and mesopelagic nautical area scattering coefficient

The total amount of scattered energy produced per square nautical mile (nmi) over a depth range is known as the nautical area scattering coefficient (NASC, s_A, $\mathrm{m}^2\ \mathrm{nmi}^{-2}$, Maclennan et al. 2002). The NASC values over the epipelagic (s_{epi}, 0–200 m) and mesopelagic (s_{meso}, 200–1000 m) zones (in 5 m depth bins in both) are given by:

$$s_{\mathrm{epi}} = \sum_{j=0}^{40} \left(\sum_{i=0}^{25} \left(\mathrm{P}_{\mathbf{z}[j],\mathbf{m}[i]} \times 10^{(\mathbf{m}[i]/10)} \right) \right) \times 4\pi \times 1852^2 \quad (3)$$

and

$$s_{\mathrm{meso}} = \sum_{j=40}^{200} \left(\sum_{i=0}^{25} \left(\mathrm{P}_{\mathbf{z}[j],\mathbf{m}[i]} \times 10^{(\mathbf{m}[i]/10)} \right) \right) \times 4\pi \times 1852^2 \quad (4)$$

respectively, where j is an index for the vector $\mathbf{z}$, which consists of 200 equally spaced SSL depth bins (0–1000 m by 5 m), and i is an index for the vector $\mathbf{m}$, which comprises 25 equally spaced SSL MVBS bins (–50 to –100 dB re 1 m^{-1} in intervals of 2 dB re 1 m^{-1}).

Principal DSL depth, MVBS and stability

The probability of observing an SSL at a specific depth, $\mathrm{P}_{\mathbf{z}[j]}$, defined as the vertical stability of an SSL, is given by:

$$\mathrm{P}_{\mathbf{z}[j]} = \sum_{i=0}^{25} \mathrm{P}_{\mathbf{z}[j],\mathbf{m}[i]} \quad (5)$$

The principal or most common DSL depth, z_{PDSL} (see Proud et al. 2017), was determined by finding the maximum value of $\mathrm{P}_{\mathbf{z}[j]}$ between 200 and 1000 m ($\mathbf{z}[40]$ to $\mathbf{z}[200]$):

$$\mathrm{P}_{\mathbf{z}[40:200]} = \{\mathrm{P}_{\mathbf{z}[40]}, \mathrm{P}_{\mathbf{z}[41]}, \mathrm{P}_{\mathbf{z}[42]} \ldots, \mathrm{P}_{\mathbf{z}[199]}\} \quad (6)$$

$$\mathrm{P}_{\mathrm{PDSL}} = max(\mathrm{P}_{\mathbf{z}[40:200]}) \quad (7)$$

$$z_{\mathrm{PDSL}} = \mathbf{z}[argmax(\mathrm{P}_{\mathbf{z}[40:200]})] \quad (8)$$

where $\mathrm{P}_{\mathrm{PDSL}}$ is the probability of observing the principal DSL defined here as DSL vertical stability, and *argmax* is a function that returns the index of the maximum value. For example, in the case where a DSL was always observed at a specific depth, $\mathrm{P}_{\mathrm{PDSL}}$ would equal 1, i.e. the DSL was always observed at z_{PDSL} and therefore had a high vertical stability. Similarly, given that a DSL has been observed, the most likely MVBS value of the principal DSL, $\mathrm{MVBS}_{\mathrm{PDSL}}$, is given by:

$$\mathrm{P}_{\mathbf{m}[i]} = \sum_{j=40}^{200} \mathrm{P}_{\mathbf{z}[j],\mathbf{m}[i]} \Bigg/ \sum_{j=40}^{200} \left(\sum_{i=0}^{25} \left(\mathrm{P}_{\mathbf{z}[j],\mathbf{m}[i]} \right) \right) \quad (9)$$

$$\mathrm{P}_{\mathbf{m}[0:25]} = \{\mathrm{P}_{\mathbf{m}[0]}, \mathrm{P}_{\mathbf{m}[1]}, \mathrm{P}_{\mathbf{m}[2]} \ldots, \mathrm{P}_{\mathbf{m}[24]}\} \quad (10)$$

$$\mathrm{P}_{\mathrm{PMVBS}} = max(\mathrm{P}_{\mathbf{m}[0:25]}) \quad (11)$$

$$\mathrm{MVBS}_{\mathrm{PDSL}} = \mathbf{m}[argmax(\mathrm{P}_{\mathbf{m}[0:25]})] \quad (12)$$

where $\mathrm{P}_{\mathrm{MVBS}}$ is the probability of the principal DSL having an MVBS value of $\mathrm{MVBS}_{\mathrm{PDSL}}$.

Clustering SPDs

A distance measure was derived to determine the similarity between each SPD. Since the SPDs were all constructed from a set of discrete probabilities, with values between 0 and 1 and with just 1 value per depth/MVBS bin, a simple matrix subtraction was used to calculate a relative distance measure:

$$\mathrm{dist}_{\mathbf{AB}} = \sum \mathrm{abs}(\mathbf{A} - \mathbf{B}) \quad (13)$$

where $\mathbf{A}$ and $\mathbf{B}$ are 2-dimensional arrays (SPDs) and $\mathrm{dist}_{\mathbf{AB}}$ is a relative distance measure between $\mathbf{A}$ and $\mathbf{B}$. The maximum value of $\mathrm{dist}_{\mathbf{AB}}$ is equal to the size of the SPD arrays (240 depth bins × 25 MVBS bins = 6000 cells), i.e. where the probability of SSL observation at a specific depth and MVBS combination in $\mathbf{A}$ = 0, the probability for the same depth and MVBS values in $\mathbf{B}$ would equal 1. By the same logic, where 2 SPDs are identical (i.e. where the probability of

observing SSLs across all depth and MVBS combinations is the same), $dist_{AB} = 0$.

Using Eq. (13), a dissimilarity matrix **D** that contained the pairwise distances between all daytime SPDs was constructed. Classical multi-dimensional scaling (MDS, Hout et al. 2013) was applied to reduce the data to a smaller number of dimensions, improving computational efficiency. From the resulting configuration matrix, an appropriate number of dimensions, was selected by evaluating values of stress (the degree of correspondence between the distances of the original data and MDS map, where a value of 0 is perfect correspondence). A *k*-means clustering algorithm (Hartigan & Wong 1979) was applied to the resultant reduced dataset to determine the natural number of groupings or clusters that were evident within the data. The optimum number of clusters was selected by identifying interruptions, or elbow-like features, in the log-likelihood (LL) trend (e.g. Sugar 1998). The algorithm was run for a range of *k* clusters (2–25), where at each step the LL value was determined (Eqs. 14 & 15) to enable model assessment:

$$P(x|u) = \frac{e^{-\sum_{d\in D}(u_d - x_d)^2}}{\sum_u e^{-\sum_{d\in D}(u_d - x_d)^2}} \quad (14)$$

$$LL = \sum_{x\in X} \log max(P(x|u)) \quad (15)$$

where x denotes an element of the set of samples X, d denotes an element of the set of dimensions D and $P(x|u)$ is the probability of sample x (i.e. a single SPD) belonging to model u (*k*-means model) and d specifies the dimension of the reduced dataset.

RSPDs

The resultant *k*-clusters, consisting of n cluster members (SPDs formed from observations made within a single 300 km × 300 km cell) were merged to form new RSPDs with larger spatial coverage (equal to n × 90 000 km^2) by matrix addition. This operation was carried out by adding the underlying data ($obs_{z,MVBS}$, see Eq. 1) for all SPDs in each cluster together, and then determining a new set of probabilities by applying new values of se_z to Eq. (1); this accounted for differences in sampling effort between cluster members. The merged clusters of SPDs (RSPDs) were associated spatially with individual cluster members. Finally, a local neighbourhood dilation filter (3 × 3 cells) was passed over the spatial grid of cells labelled by cluster number (*k*), and the centre value of the filter (either a cluster number or an unlabelled cell) was replaced with the maximum value calculated over the local neighbourhood. This filtering process removed anomalies and smoothed spatial transitions between RSPDs.

RESULTS

In total, 39 455 SSLs were extracted from the acoustic survey data via the SSLEM (Proud et al. 2015), including 26 474 DSLs, and summarised by a set of metrics (depth, thickness and MVBS). The SSL metrics were split by day and night and assigned to 297 unique 300 km × 300 km cells (these equate to ca. 9 % of the surface of the global open ocean where seabed depth >1000 m). SSL probability distributions (SPDs) were determined for each cell, and a distance measure was computed resulting in a dissimilarity matrix, **D**, with 297 rows and columns. The MDS analysis of **D** indicated that for a stress value of 0.1 (Kruskal 1964), **D** could be reduced from 297 dimensions to 37. The lower dimensional representation of the data, **D′**, accounted for 72 % of the variance.

k-means clustering was applied to **D′** and, using calculated values of the LL (Eq. 15), a 6-cluster model was selected. An elbow-like feature was apparent at 6 clusters (Fig. 1), increasing the value of the LL away from the otherwise decreasing trend of LL with *k* clusters; this feature indicated that there was a better than expected fit at this scale. As the number of clusters increased, particularly towards 15, more of these elbow-like features appeared. Since in this

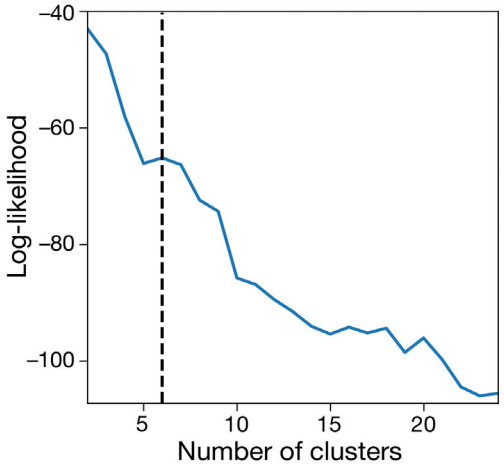

Fig. 1. Change in log-likelihoods (LLs) by number of *k*-means clusters. Six clusters were selected (indicated by the black dashed line) on the basis that an elbow-like feature with an increasing LL at that scale diverged from the otherwise decreasing linear trend

study we were interested in regional-scale trends, taking the first natural grouping was appropriate. For the 6-cluster model, 89% of the SPDs were assigned to a cluster with a probability (Eq. 14) that was at least twice the value of the next best selection, indicating a good fit.

DSL vertical stability and sampling effort of SPD cluster members

Sampling effort per SPD ranged between ca. 1 and 175 h, and DSL vertical stability (P_{PDSL}) ranged between ca. 0.32 and 1 (Fig. 2). DSLs were typically less stable at night than during the day, and the lowest values of DSL vertical stability occurred in summer (Fig. 2). DSLs in clusters 1, 2, 4 and 5 were the most vertically stable, whereas DSLs in cluster 6 were highly unstable across the full range of sampling effort values.

Geographical distribution of SPD clusters

The SPD cluster members were plotted in space, revealing the underlying spatial affiliation of the echosounder observations (Fig. 3). The clusters formed large-scale spatially aggregated regions (Fig. 3). Cluster 6 was located mostly at higher latitudes, typically lying poleward of 40° latitude in both hemispheres. Cluster 4 was mainly composed of a single region within the south Indian Ocean. The other clusters occurred at mid to low latitudes, forming sub-regions both north and south of the equator (Fig. 3).

RSPDs

SPDs were merged by cluster to form 6 distinct RSPDs (Fig. 4). RSPDs 1 to 5 exhibited strong compact trunk-like features in depth–MVBS space (Fig. 4). MVBS values of these RSPDs varied by a factor of 10 from RSPD1 ($MVBS_{PDSL}$ = −67 dB re 1 m^{-1}) to RSPD5 ($MVBS_{PDSL}$ = −77 dB re 1 m^{-1}). There was also an increase in backscattering intensity from day to night at the surface and a decrease in the mesopelagic depth zone, indicating DVM (Table 1).

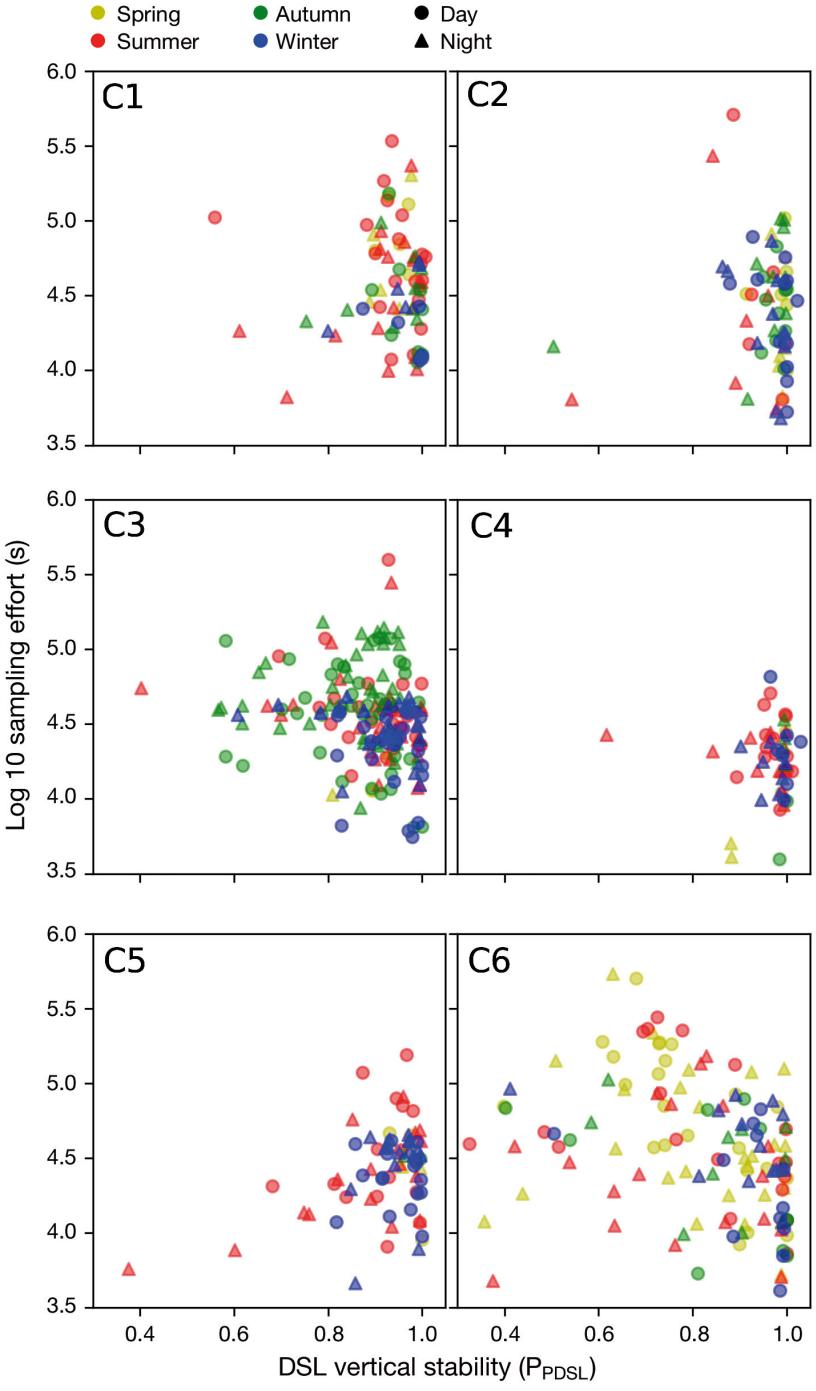

Fig. 2. Deep scattering layer (DSL) vertical stability, defined as the maximum probability of DSL observation (P_{PDSL}) and sampling effort (echosounder observations) by season, diel state and cluster (C1 to C6) for each local-scale (300 km × 300 km cell) sound scattering layer probability distribution

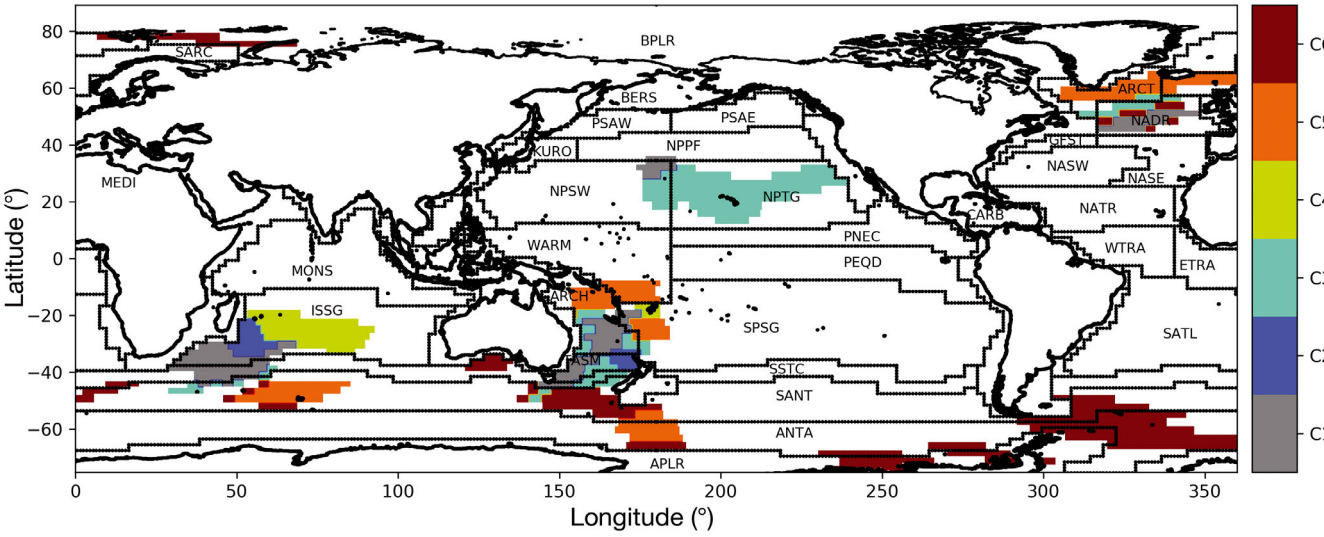

Fig. 3. Geographical distribution of echosounder data (coloured cells) and sound scattering layer probability distribution cluster membership (C1 to C6). Longhurst's (2007) pelagic ocean provinces are shown for reference, labelled by their short name

All RSPDs had relatively stable depth structures during both day and night (Fig. 4), i.e. in all regions there was a component of the DSL assemblage that did not migrate, suggesting that 'resident' night-time DSLs are a ubiquitous feature of open-ocean pelagic ecosystems. This phenomenon could be explained by a component of the DSL consisting of either a temporary (e.g. through ontogenetic migration) or per-

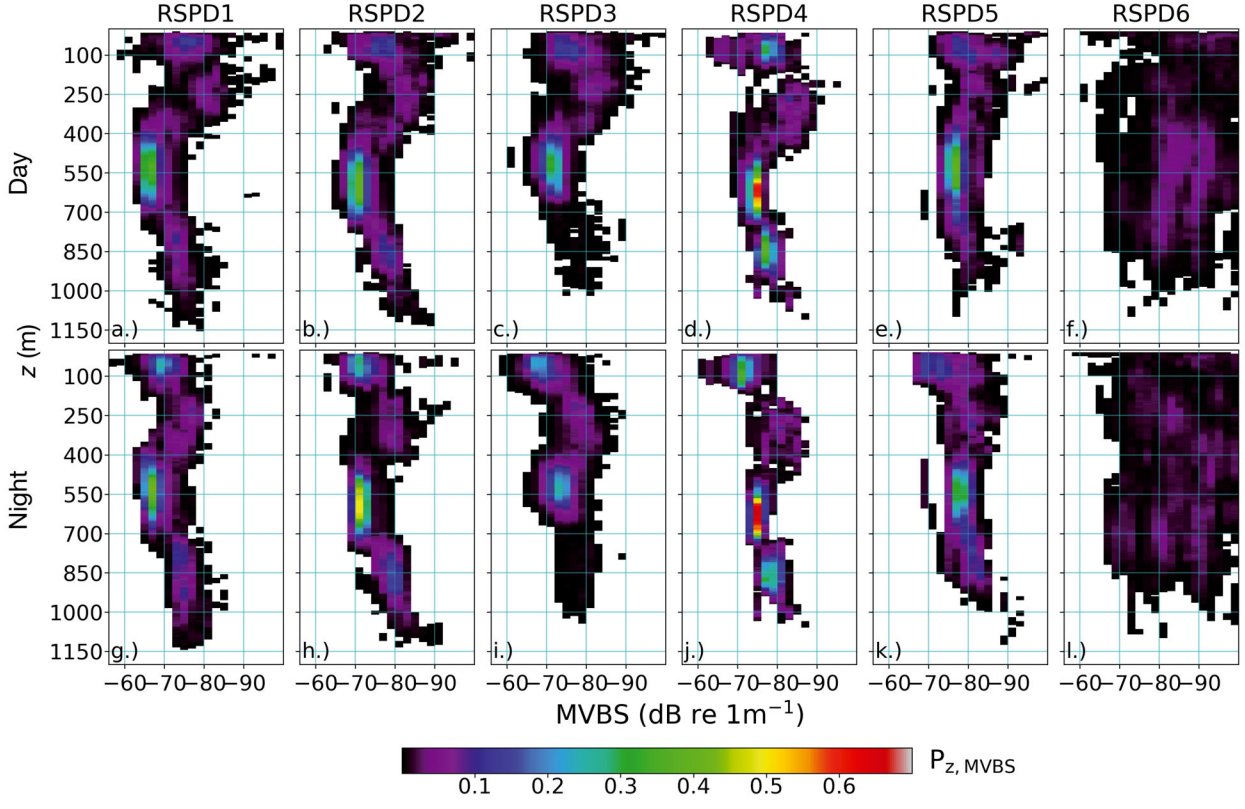

Fig. 4. Regional-scale sound scattering layer probability distributions (RSPDs) plotted in depth–mean volume backscattering strength (MVBS) space. Each RSPD has a day and night component. $P_{z,MVBS}$ is the probability of observing a sound scattering layer of a given depth (z) and MVBS value. White regions indicate a probability of 0, i.e. no sound scattering layers were observed in the region represented by the RSPD for those specific depth–MVBS combinations

Table 1. Regional-scale sound scattering layer (SSL) probability distribution (RSPD) characteristics ranked in accordance to their daytime s_{meso} values. SCI: seasonal coverage index, which ranges from 1 (single season) to 4 (all seasons uniformly represented); z_{PDSL}: principal (most common) deep scattering layer (DSL; SSL deeper than 200 m) depth; $MVBS_{PDSL}$: most likely mean volume backscattering strength (MVBS) value for the principal DSL, given that a DSL is observed; and s_{meso} and s_{epi}: nautical area scattering coefficient (NASC) values for SSLs found within the mesopelagic (200–1000 m) and epipelagic (0–200 m) zones, respectively. Stability values of principal DSL depth (P_{PDSL}) and principal DSL MVBS (P_{PMVBS}) are given in brackets. nmi: nautical mile

RSPD	SCI (1–4)	Day				Night			
		z_{PDSL} (m)	$MVBS_{PDSL}$ (dB re 1 m^{-1})	s_{meso} (m^2 nmi^{-2})	s_{epi} (m^2 nmi^{-2})	z_{PDSL} (m)	$MVBS_{PDSL}$ (dB re 1 m^{-1})	s_{meso} (m^2 nmi^{-2})	s_{epi} (m^2 nmi^{-2})
1	2.1	510 (0.87)	−67 (0.23)	2692[a]	139[a]	525 (0.91)	−67 (0.27)	2173[a]	479[a]
2	2.9	590 (0.94)	−71 (0.25)	1103[a]	143[a]	585 (0.93)	−71 (0.33)	848[a]	368[a]
3	1.7	510 (0.82)	−73 (0.25)	679[a]	121[a]	510 (0.77)	−73 (0.2)	390[a]	650[a]
4	3.1	615 (0.95)	−75 (0.31)	517[a]	232[a]	605 (0.97)	−75 (0.31)	370[a]	511[a]
5	1.8	530 (0.87)	−77 (0.35)	287[a]	44[a]	545 (0.85)	−79 (0.26)	215[a]	280[a]
6	1.8	625 (0.44)	−83 (0.12)	95	19	615 (0.46)	−91 (0.09)	152	35

[a]Day-to-night increase in NASC in the epipelagic and decrease in the mesopelagic implies diel vertical migration (DVM)

manent (e.g. non-migrating fish species) resident mesopelagic community, or by asynchronous vertical migration (e.g. Dupont et al. 2009) where individuals of a given species behave as individuals, each selectively undertaking migration (intermittently or opportunistically) at a time cued by some individual trigger (e.g. nutritional state).

RSPD6, by contrast, was characterised by a broad, shallow probability distribution (Fig. 4), i.e. SSLs varied substantially in both depth and MVBS, and there was no common structure. This RSPD arises in an area with seasonally-limited sampling, so is not an artefact caused by blurring of temporal variability (Table 1, SCI = 1.8). It is formed from cells with low DSL vertical stability (Fig. 2) and cells that contain relatively low MVBS SSLs (<−85 dB re 1 m^{-1}, see Fig. 4). RSPD6 MVBS increased from day to night in the mesopelagic (Table 1).

Depth structure and DSL stability of RSPDs

RSPDs were ranked by s_{meso}, which is reflected by the decreasing value of $MVBS_{PDSL}$ (Table 1 and Fig. 5) from RSPD1 to 6. Analysis of the mesopelagic depth structure (number and depth of DSLs) and DSL vertical stability ($P_{z[40\text{-}200]}$, see Eq. 5), enabled categorisation of the RSPDs into 3 DSL types: (1) single-shallow DSL (SS-DSL: RSPD1, 3 and 5), i.e. a single DSL at ca. 500 m; (2) double-deep DSL (DD-DSL: RSPD2 and 4), i.e. 2 DSLs at ca. 600 and 850 m; and (3) unclassified DSL (U-DSL: RSPD6), with highly variable depth structure and/or low (<−85 dB re 1 m^{-1}) MVBS values (Table 1, Figs. 2, 4 & 5).

DISCUSSION

The RSPDs defined here give new insight into fine-scale (10s of m) depth structure of open-ocean communities and their day-to-night vertical stability (i.e. probability of observation at depth) and MVBS variability. They provide evidence that regional-scale spatially coherent community depth structures exist between 0 and 1200 m (Figs. 3 & 4). Given that DSL metrics (e.g. z_{PDSL} and $MVBS_{PDSL}$, see Table 1) are characteristics of the underlying mesopelagic biological communities and that similar partitions arise from environmentally based regionalisations (e.g. Longhurst provinces), then the observed cohesion here is likely to be due to environmental control. The between-region differences in DSL vertical stability and MVBS variability (Figs. 2, 4 & 5) are not artefacts of uneven sampling effort (see SCI in Table 1 and Fig. 2). The most vertically stable region was RSPD4 (defined by the highest P_{PDSL} values, see Table 1) which occurred in the Southern Indian Ocean (Fig. 3), the area for which we have full seasonal sampling coverage (Table 1, SCI = 3.1). Conversely, the high vertical instability in the polar regions was evident in our seasonally restricted data (we do not have data for the logistically challenging winter period, see Table 1, RSPD6, SCI = 1.8). All RSPDs include resident night-time DSLs which adhere to their daytime depth (Fig. 4).

Spatial variability in DSL number and fine-scale depth structure will impact predator–prey interactions in pelagic food webs and carbon transfer in the water column via the BCP (Klevjer et al. 2016).

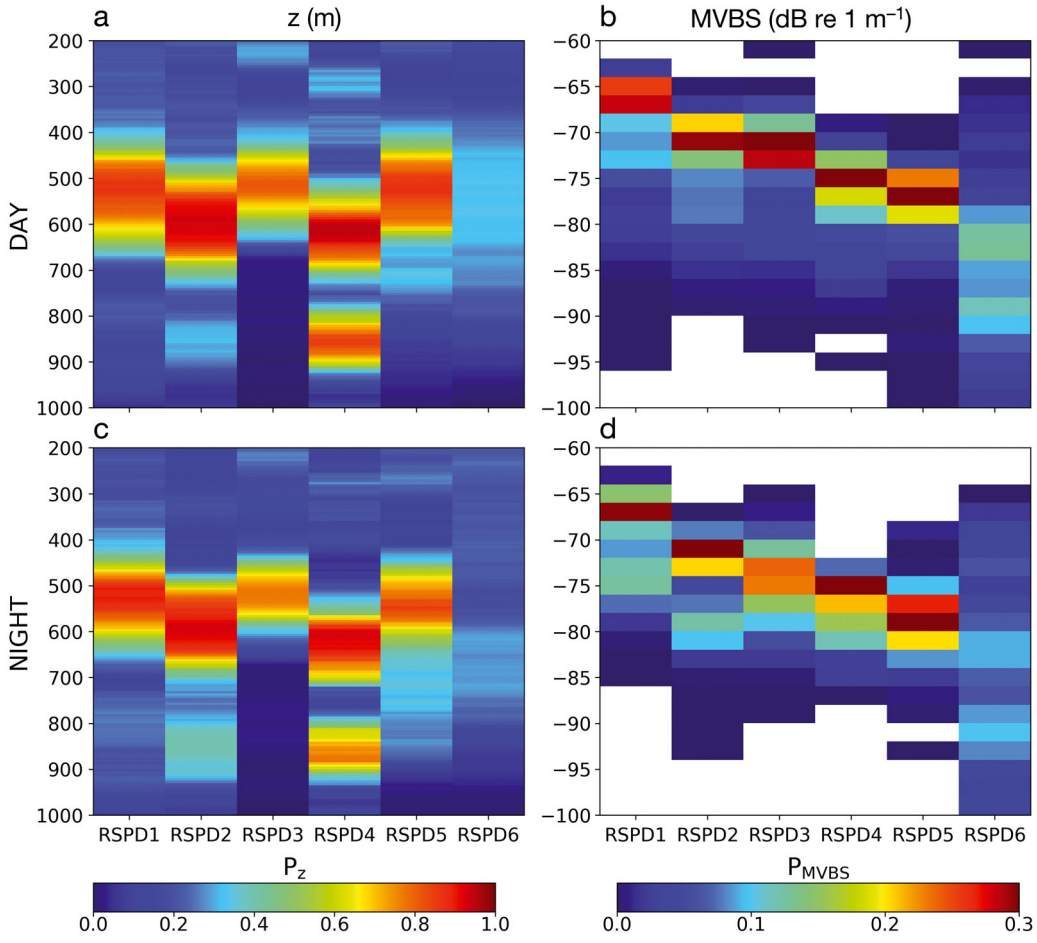

Fig. 5. Stability of deep scattering layer (DSL; sound scattering layer deeper than 200 m) depth and mean volume backscattering strength (MVBS) for each regional-scale sound scattering layer probability distribution (RSPD). (a,c) P_z is the probability of DSL observation by depth; (b,d) P_{MVBS} is the probability of an observed DSL having a specific MVBS value

Such variability should be considered in ocean partitioning schemes and in the design of mesopelagic components of ecosystem and biogeochemical models.

Implications for predator–prey interactions

DSL inhabitants (e.g. micronektic organisms such as mesopelagic fish) represent a potentially rich food resource for epipelagic predators (e.g. southern bluefin tuna *Thunnus maccoyii* and Pacific bluefin tuna *T. orientalis*; Bestley et al. 2008) at night and deep-sea consumers during the day (Hazen & Johnston 2010). Variability in daytime and night-time depth of DSLs, spatially characterised by RSPDs (Fig. 4), will likely impact the energy budgets of their inhabitants and deep-diving air-breathing predators (e.g. southern elephant seals *Mirounga leonina* for which DSLs constitute a dynamic prey landscape; Boersch-Supan et al. 2012). For active vertical migrators, the opportunity to feed (and digest) in shallow, warm and productive waters may bring metabolic advantages that outweigh the cost of migration. For predators, however, the fact that potential prey biomass migrates deep during the day may effectively take it out of their reach: prey may exist but may be inaccessible.

Predators adjust the time allocated to foraging according to the prey patch quality (Schoener 1979, Mori & Boyd 2004). Deep-diving air-breathing predators that are constrained by their oxygen requirements have been observed to rely on spatially predictable foraging grounds (Brown 1980, Charrassin & Bost 2001). Variation in prey availability leads predators to adjust their foraging behaviour and/or location, affecting their foraging success, which in turn has an impact on survival, breeding success and

eventually population abundance (New et al. 2014). Mesopelagic fish, which are a key component of the DSL, are an important prey item for king penguins and southern elephant seals (Olsson & North 1997, Vacquié-Garcia et al. 2015). Both southern elephant seals and king penguins routinely dive to depths coincident with the DSL, although direct evidence for foraging on DSLs by these species remains lacking. King penguins can dive to depths of ca. 400 m (Charrassin et al. 2002), and southern elephant seals have dive ranges beyond the mesopelagic zone (down to 2000 m; McIntyre et al. 2010). If these predators do feed upon DSLs, variation in DSL depth will impact the energy expenditure of their dives.

The daytime vertical range of DSLs in RSPD1, 3 and 5 extends to ca. 400 m at their shallowest extent, whereas in RSPD2 and 4, DSLs reside slightly deeper at their shallowest extent (ca. 500 m, see Fig. 4). Geographically, the only RSPDs within the latitudinal feeding range of king penguins (i.e. south of the polar front) are the shallower DSLs (e.g. RSPD5; see Fig. 3). It is perhaps no coincidence that at just beyond the maximum extent of the king penguins' diving range, prey biomass starts to increase because predation pressure upon DSL occupants is reduced. Vertical zonation is a common phenomenon in the marine realm. The most readily apparent examples come from the intertidal, where the lower depth distributions of many species are set by predation (e.g. Luckens 1975). On land, vivid evidence of the impact of consumption on vertical distribution is seen by the browsing of giraffes on trees (Woolnough & Du Toit 2001). However, although the probability of DSL observation at shallower depths is low in RSPD1, 3 and 5 (Fig. 4), they have been observed on occasion (<10% probability), and we have sampled from an incomplete dataset both temporally (e.g. missing winter period in the Southern Ocean) and spatially (e.g. missing large sections of the Atlantic and eastern boundary upwelling systems).

The energy consumption by mesopelagic organisms that actively migrate can be divided into 4 different energy-consuming activities: (1) foraging at the surface during the night (e.g. Dypvik & Kaartvedt 2013); (2) buoyancy control, via a gas bladder, lipid investment or by swimming (Proud et al. 2018); (3) predator evasion (Hays 2003); and (4) actively swimming during vertical migration (Brierley 2014). Variability in DSL depth directly impacts activities (2)–(4) to different degrees. For example, a gas-bladdered fish would need to produce more gas to re-inflate its bladder to recover neutral buoyancy after moving from a depth of 500 m down to 600 m (e.g. from RSPD1 to RSPD2). The fish may achieve reduced predation from above by adopting a deeper depth (becoming inaccessible to some predators e.g. king penguins) but has an energetic cost for this, and will also expend more energy to vertically migrate upwards to its feeding depth. Foraging will also be impacted indirectly, as the energy remaining after other activities (2–4 above) may limit energy availability for foraging. To investigate further, fine-scale predator–prey studies between depth-restricted predators and DSLs should be conducted.

Low DSL vertical stability in polar regions

We have revealed 2 different DSL depth structures, i.e. SS-DSL and DD-DSL. The remaining cluster, RSPD6, found mainly in polar regions (Fig. 3), consisted of SPDs with low DSL vertical stability (Fig. 2) and relatively low-intensity scattering layers (Fig. 4). Polar regions are cold, metabolic rates are reduced, and life cycle stages are longer, reducing survival probability of larvae and hence lowering trophic efficiency (Rogers et al. 2012). Relatively few mesopelagic fish species inhabit the polar regions (3 species of Myctophidae in the Arctic and 19 in the Antarctic compared with >100 species in the Indian Ocean, www.fishbase.org), which may lead to reduced productivity and ecosystem stability (Johnson et al. 1996). As the climate warms, fish diversity in polar regions may increase (e.g. Kaartvedt & Titelman 2018) and, with it, ecosystem stability and biomass may increase. In the Southern Ocean, a proportion of the fish population is believed to be migratory, spending their early life-cycle stages equatorward of the polar front (Saunders et al. 2017) and progressing towards the Antarctic shelf as adults, following Bergmann's Rule (Saunders & Tarling 2018). Since fish are relatively strong scatterers compared with zooplankton (Lavery et al. 2007), high spatial and temporal variability in community composition (proportion of zooplankton to fish) and biomass, along with patchy immigrations, could lead to the observed low vertical stability in DSL depth (see Table 1 and Fig. 2) and high variability in MVBS (Fig. 4, RSPD6).

Partitioning the ocean

The spatial coherence of the clusters (see Fig. 3) provides evidence that pelagic communities as described using SSL characteristics (z, MVBS etc.) are

distinct at the regional scale. This is particularly apparent in the south Indian Ocean region, where even though the underlying data had the most extensive seasonal coverage (Table 1, RSPD4, SCI = 3.1), spatially coherent regions formed. The spatial extent of the RSPDs varied geographically. Across the North Atlantic, for example, the SSL structure varied substantially, shifting between 4 different RSPDs over a relatively small distance (Fig. 3). Anderson et al. (2005) reported similar findings, observing high spatial and seasonal variability in DSL depth and echo intensity, inferring that changes in oceanographic regimes were responsible. Conversely, in the North Pacific, the SSL structure was more spatially stable, formed in the majority of a single RSPD (Fig. 3).

Flynn & Marshall (2013) described 4 zoogeographic regions off eastern Australia based on lanternfish species occurrence data and environmental variables (nitrate, phosphate, oxygen, salinity and temperature). The 4 regions, i.e. Coral Sea, Subtropical Lower water, Subantarctic and Subtropical Convergence zone (South Tasman region), correspond spatially to our RSPD5, 3, 6 and 1, respectively (our Fig. 3, and see Fig. 7 of Flynn & Marshall 2013). There is a stark difference between the Subantarctic region (RSPD6), also defined by Longhurst (2007) as the Subantarctic water ring (SANT in Fig. 3), and the other 3 RSPDs/zoogeographic regions, which all fall into the SS-DSL depth structure type and are not as well defined (Flynn & Marshall 2013, their Fig. 7). In the bioregionalisation model of Flynn & Marshall (2013), latitude is a significant covariate, and they suggested that this is a proxy for some unknown parameter, speculating that it could be related to food source distribution, breeding, competitive exclusion or a consequence of larval transport barriers or aggregating eddies. Here, the RSPDs are distinguished by their DSL echo intensity, which increases from RSPD1 to RSPD6 (Table 1). This increase could be related to an increase in biomass (Irigoien et al. 2014), and therefore related to food source distribution, or may just be a consequence of differences in fish population scattering properties (Davison et al. 2015).

Recently, Proud et al. (2017), described a mesopelagic biogeography based on the daytime depth of the principal DSL and 38 kHz backscattering intensity of observed daytime DSLs. They predicted global mesopelagic backscatter using a simple linear model in which the product of PP and temperature at the depth of the principal DSL was used as a predictor variable. In this study, we have defined RSPDs based on the full water-column SSL structure (not just the depth of the principal DSL), and quantified vertical stability of these structures. By including consideration of the full water-column structure, ecological partitions could be constructed that are more suitable for studies where fine-scale distribution of DSLs is required, e.g. foraging behaviour of deep-diving predators such as elephant seals and king penguins in the Southern Ocean (Boersch-Supan et al. 2012).

Mesopelagic components in ecosystem models

Recognition of the importance of the role of DVM in the carbon cycle has increased over the last decade (Van De Waal et al. 2010, Doney et al. 2012, Passow & Carlson 2012, Giering et al. 2014, Mitra et al. 2014), but modelling of these processes at fine scales has not developed as quickly. Traditional ecological models such as Ecopath (Christensen & Walters 2004) do not explicitly define depth structure. Newer, more complex models such as Atlantis (Fulton et al. 2011) have both diel variability and integrated depth levels. Modellers are now beginning to adapt their models. For example, SEAPOYDM (Lehodey et al. 2008) has recently been updated to included DVM behaviour and consideration of DSL depth structure related to euphotic depth (Lehodey et al. 2015). Accurate representation of the BCP in these models is important because output from these models feeds into climate/Earth-system models.

Conclusions

Regional-scale, spatially and vertically coherent, water-column community depth structures can be derived from echosounder observations. In total, we have described 6 RSPDs from a near-global acoustic dataset. Other characteristic SSL depth structures may exist in regions for which we had no observations, e.g. in the central and South Atlantic and the eastern boundary upwelling systems. Variability in DSL number, depth, MVBS and vertical stability drive the characteristic forms of these day–night depth structures (SS-DSL and DD-DSL), and these forms will likely impact the efficiency of the BCP and predator–prey interactions. The results presented here highlight the variability in fine-scale depth structure and vertical stability of the mesopelagic community throughout the global ocean. Both of these should be considered when partitioning the ocean's water column into bioregions, and in the future development of ecological models.

Acknowledgements. We thank the British Oceanographic Data Centre, the Australian Integrated Marine Observing System, the British Antarctic Survey, and Dr. Phil Hosegood for providing echosounder data. This study received support from the European H2020 International Cooperation project MESOPP (Mesopelagic Southern Ocean Prey and Predators, www.mesopp.eu/).

LITERATURE CITED

Aksnes DL, Røstad A, Kaartvedt S, Martinez U, Duarte CM, Irigoien X (2017) Light penetration structures the deep acoustic scattering layers in the global ocean. Sci Adv 3: e1602468

Alvarino A (1965) Chaetognaths. Oceanogr Mar Biol Annu Rev 3:115–194

Anderson CIH, Brierley AS, Armstrong F (2005) Spatio-temporal variability in the distribution of epi- and mesopelagic acoustic backscatter in the Irminger Sea, North Atlantic, with implications for predation on *Calanus finmarchicus*. Mar Biol 146:1177–1188

Anderson TR, Martin AP, Lampitt RS, Trueman CN, Henson SA, Mayor DJ (2018) Quantifying carbon fluxes from primary production to mesopelagic fish using a simple food web model. ICES J Mar Sci, https://doi.org/10.1093/icesjms/fsx234

Andreeva IB, Galybin NN, Tarasov LL (2000) Vertical structure of the acoustic characteristics of deep scattering layers in the ocean. Acoust Phys 46:505–510

BAS (British Antarctic Survey) (2015) Raw acoustic data collected by ship-borne EK60 echo sounder in the Scotia Sea (Oct–Dec 2006; Feb–Apr 2008; Mar–Apr 2009). Polar Data Centre; British Antarctic Survey, Natural Environment Research Council, Cambridge

Bestley S, Patterson TA, Hindell MA, Gunn JS (2008) Feeding ecology of wild migratory tunas revealed by archival tag records of visceral warming. J Anim Ecol 77: 1223–1233

Bianchi D, Mislan KAS (2016) Global patterns of diel vertical migration times and velocities from acoustic data. Limnol Oceanogr 61:353–364

Bianchi D, Galbraith ED, Carozza DA, Mislan KAS, Stock CA (2013) Intensification of open-ocean oxygen depletion by vertically migrating animals. Nat Geosci 6: 545–548

Boersch-Supan PH, Boehme L, Read JF, Rogers AD, Brierley AS (2012) Elephant seal foraging dives track prey distribution, not temperature: comment on McIntyre et al. (2011). Mar Ecol Prog Ser 461:293–298

Boyce DG, Lewis MR, Worm B (2010) Global phytoplankton decline over the past century. Nature 466:591–596

Boyce DG, Lewis MR, Worm B (2012) Integrating global chlorophyll data from 1890 to 2010. Limnol Oceanogr Methods 10:840–852

Brierley AS (2014) Diel vertical migration. Curr Biol 24: R1074–R1076

Briggs J (1974) Marine zoogeography. McGraw-Hill, New York, NY

Brinton E (1962) The distribution of Pacific euphausiids. Bull Scripps Inst Oceanogr Univ Calif 8:51–270

Brown RGB (1980) Seabirds as marine animals. In: Burger J, Olla BL, Winn HE (eds) Behavior of marine animals. Plenum Press, New York, NY, p 1–39

Charrassin JB, Bost CA (2001) Utilisation of the oceanic habitat by king penguins over the annual cycle. Mar Ecol Prog Ser 221:285–298

Charrassin JB, Le Maho Y, Bost CA (2002) Seasonal changes in the diving parameters of king penguins (*Aptenodytes patagonicus*). Mar Biol 141:581–589

Christensen V, Walters CJ (2004) Ecopath with Ecosim: methods, capabilities and limitations. Ecol Model 172: 109–139

Davison PC, Koslow JA, Kloser RJ (2015) Acoustic biomass estimation of mesopelagic fish: backscattering from individuals, populations, and communities. ICES J Mar Sci 72:1413–1424

Doney SC, Ruckelshaus M, Duffy JE, Barry JP and others (2012) Climate change impacts on marine ecosystems. Annu Rev Mar Sci 4:11–37

Dupont N, Klevjer TA, Kaartvedt S, Aksnes DL (2009) Diel vertical migration of the deep-water jellyfish *Periphylla periphylla* simulated as individual responses to absolute light intensity. Limnol Oceanogr 54:1765–1775

Dypvik E, Kaartvedt S (2013) Vertical migration and diel feeding periodicity of the skinnycheek lanternfish (*Benthosema pterotum*) in the Red Sea. Deep Sea Res I 72: 9–16

Fennell S, Rose G (2015) Oceanographic influences on deep scattering layers across the North Atlantic. Deep Sea Res I 105:132–141

Flynn AJ, Kloser RJ (2012) Cross-basin heterogeneity in lanternfish (family Myctophidae) assemblages and isotopic niches ($\delta^{13}C$ and $\delta^{15}N$) in the southern Tasman Sea abyssal basin. Deep Sea Res I 69:113–127

Flynn AJ, Marshall NJ (2013) Lanternfish (Myctophidae) zoogeography off eastern Australia: a comparison with physicochemical biogeography. PLOS ONE 8:e80950

Fulton EA, Link JS, Kaplan IC, Savina-Rolland M and others (2011) Lessons in modelling and management of marine ecosystems: the Atlantis experience. Fish Fish 12: 171–188

Giering SLC, Sanders R, Lampitt RS, Anderson TR and others (2014) Reconciliation of the carbon budget in the ocean's twilight zone. Nature 507:480–483

Godø OR, Samuelsen A, Macaulay GJ, Patel R and others (2012) Mesoscale eddies are oases for higher trophic marine life. PLOS ONE 7:e30161

Hartigan JA, Wong MA (1979) Algorithm AS 136: a *K*-means clustering algorithm. J R Stat Soc Ser C Appl Stat 28: 100–108

Hays GC (2003) A review of the adaptive significance and ecosystem consequences of zooplankton diel vertical migrations. Hydrobiologia 503:163–170

Hazen EL, Johnston DW (2010) Meridional patterns in the deep scattering layers and top predator distribution in the central equatorial Pacific. Fish Oceanogr 19: 427–433

Hout MC, Papesh MH, Goldinger SD (2013) Multidimensional scaling. Wiley Interdiscip Rev Cogn Sci 4:93–103

Irigoien X, Klevjer TA, Røstad A, Martinez U and others (2014) Large mesopelagic fishes biomass and trophic efficiency in the open ocean. Nat Commun 5:3271

Johnson KH, Vogt KA, Clark HJ, Schmitz OJ, Vogt DJ (1996) Biodiversity and the productivity and stability of ecosystems. Trends Ecol Evol 11:372–377

Jónasdóttir SH, Visser AW, Richardson K, Heath MR (2015) Seasonal copepod lipid pump promotes carbon sequestration in the deep North Atlantic. Proc Natl Acad Sci USA 112:12122–12126

Kaartvedt S, Titelman J (2018) Planktivorous fish in a future Arctic Ocean of changing ice and unchanged photoperiod. ICES J Mar Sci (in press), https://doi.org/10.1093/icesjms/fsx248

Klevjer TA, Torres DJ, Kaartvedt S (2012) Distribution and diel vertical movements of mesopelagic scattering layers in the Red Sea. Mar Biol 159:1833–1841

Klevjer TA, Irigoien X, Røstad A, Fraile-Nuez E, Benítez-Barrios VM, Kaartvedt S (2016) Large scale patterns in vertical distribution and behaviour of mesopelagic scattering layers. Sci Rep 6:19873

Kloser RJ, Ryan TE, Young JW, Lewis ME (2009) Acoustic observations of micronekton fish on the scale of an ocean basin: potential and challenges. ICES J Mar Sci 66: 998–1006

Knutsen T, Wiebe PH, Gjøsæter H, Ingvaldsen RB, Lien G (2017) High latitude epipelagic and mesopelagic scattering layers — a reference for future Arctic ecosystem change. Front Mar Sci 4:1–21

Koslow JA, Kloser RJ, Williams A (1997) Pelagic biomass and community structure over the mid-continental slope off southeastern Australia based upon acoustic and midwater trawl sampling. Mar Ecol Prog Ser 146:21–35

Kruskal JB (1964) Multidimensional scaling by optimizing goodness of fit to a nonmetric hypothesis. Psychometrika 29:1–27

Lavery AC, Wiebe PH, Stanton TK, Lawson GL, Benfield MC, Copley N (2007) Determining dominant scatterers of sound in mixed zooplankton populations. J Acoust Soc Am 122:3304–3326

Lehodey P, Senina I, Murtugudde R (2008) A spatial ecosystem and populations dynamics model (SEAPODYM) — modeling of tuna and tuna-like populations. Prog Oceanogr 78:304–318

Lehodey P, Conchon A, Senina I, Domokos R and others (2015) Optimization of a micronekton model with acoustic data. ICES J Mar Sci 72:1399–1412

Longhurst AR (2007) Ecological geography of the sea, 2nd edn. Academic Press, San Diego, CA

Luckens PA (1975) Predation and intertidal zonation of barnacles at Leigh, New Zealand. N Z J Mar Freshw Res 9:355–378

Maclennan DN, Fernandes PG, Dalen J (2002) A consistent approach to definitions and symbols in fisheries acoustics. ICES J Mar Sci 59:365–369

McIntyre T, de Bruyn PJN, Ansorge IJ, Bester MN, Bornemann H, Plötz J, Tosh CA (2010) A lifetime at depth: vertical distribution of southern elephant seals in the water column. Polar Biol 33:1037–1048

Mitra A, Flynn KJ, Burkholder JM, Berge T and others (2014) The role of mixotrophic protists in the biological carbon pump. Biogeosciences 11:995–1005

Mori Y, Boyd IL (2004) The behavioral basis for nonlinear functional responses and optimal foraging in Antarctic fur seals. Ecology 85:398–410

New LF, Clark JS, Costa DP, Fleishman E and others (2014) Using short-term measures of behaviour to estimate long-term fitness of southern elephant seals. Mar Ecol Prog Ser 496:99–108

Oliver MJ, Irwin AJ (2008) Objective global ocean biogeographic provinces. Geophys Res Lett 35:L15601

Olsson O, North AW (1997) Diet of the king penguin *Aptenodytes patagonicus* during three summers at South Georgia. Ibis 139:504–512

Parekh P, Dutkiewicz S, Follows MJ, Ito T (2006) Atmospheric carbon dioxide in a less dusty world. Geophys Res Lett 33:L03610

Passow U, Carlson CA (2012) The biological pump in a high CO_2 world. Mar Ecol Prog Ser 470:249–271

Proud R, Cox MJ, Wotherspoon S, Brierley AS (2015) A method for identifying sound scattering layers and extracting key characteristics. Methods Ecol Evol 6: 1190–1198

Proud R, Cox MJ, Brierley AS (2017) Biogeography of the global ocean's mesopelagic zone. Curr Biol 27:113–119

Proud R, Handegard NO, Kloser RJ, Cox MJ, Brierley AS (2018) From siphonophores to deep scattering layers: uncertainty ranges for the estimation of global mesopelagic fish biomass. ICES J Mar Sci, doi:10.1093/icesjms/fsy037

Rogers AD, Johnston NM, Murphy EJ, Clarke A (eds) (2012) Antarctic ecosystems. John Wiley & Sons, Chichester

Saunders RA, Tarling GA (2018) Southern Ocean mesopelagic fish comply with Bergmann's Rule. Am Nat 191: 343–351

Saunders RA, Collins MA, Stowasser G, Tarling GA (2017) Southern Ocean mesopelagic fish communities in the Scotia Sea are sustained by mass immigration. Mar Ecol Prog Ser 569:173–185

Sayre RG, Wright DJ, Breyer SP, Butler KA and others (2017) A three-dimensional mapping of the ocean based on environmental data. Oceanography 30:90–103

Scheffer A, Trathan PN, Collins M (2010) Foraging behaviour of king penguins (*Aptenodytes patagonicus*) in relation to predictable mesoscale oceanographic features in the Polar Front Zone to the north of South Georgia. Prog Oceanogr 86:232–245

Schnetzer A, Steinberg DK (2002) Active transport of particulate organic carbon and nitrogen by vertically migrating zooplankton in the Sargasso Sea. Mar Ecol Prog Ser 234:71–84

Schoener TW (1979) Generality of the size-distance relation in models of optimal feeding. Am Nat 114:902–914

Scott F, Blanchard JL, Andersen KH (2014) mizer: an R package for multispecies, trait-based and community size spectrum ecological modelling. Methods Ecol Evol 5: 1121–1125

Semina HJ (1997) An outline of the geographical distribution of oceanic phytoplankton. Adv Mar Biol 32: 527–563

Spalding MD, Agostini VN, Rice J, Grant SM (2012) Pelagic provinces of the world: a biogeographic classification of the world's surface pelagic waters. Ocean Coast Manag 60:19–30

Sugar C (1998) Techniques for clustering and classification with applications to medical problems. Stanford University, Stanford, CA

Sutton TT, Clark MR, Dunn DC, Halpin PN and others (2017) A global biogeographic classification of the mesopelagic zone. Deep Sea Res Part I Oceanogr Res Pap 126: 85–102

Trebilco R, Baum JK, Salomon AK, Dulvy NK (2013) Ecosystem ecology: size-based constraints on the pyramids of life. Trends Ecol Evol 28:423–431

UNESCO (United Nations Educational, Scientific and Cultural Organization) (2009) Global Open Oceans and Deep Seabed (GOODS) — biogeographic classification. IOC Tech Ser 84. UNESCO-IOC, Paris

Vacquié-Garcia J, Guinet C, Laurent C, Bailleul F (2015) Delineation of the southern elephant seal's main forag-

ing environments defined by temperature and light conditions. Deep Sea Res Part II Top Stud Oceanogr 113: 145–153

Van De Waal DB, Verschoor AM, Verspagen JMH, Van Donk E, Huisman J (2010) Climate-driven changes in the ecological stoichiometry of aquatic ecosystems. Front Ecol Environ 8:145–152

Vinogradov M (1968) Vertical distribution of oceanic zooplankton. Acad Nauk SSSR Inst Oceanolog Moscow. (Translated by the Israel Program for Scientific Translation Ltd, Jerusalem, Keter Press, 1970)

Watling L, Guinotte J, Clark MR, Smith CR (2013) A proposed biogeography of the deep ocean floor. Prog Oceanogr 111:91–112

Woolnough A, Du Toit J (2001) Vertical zonation of browse quality in tree canopies exposed to a size-structured guild of African browsing ungulates. Oecologia 129: 585–590

Editorial responsibility: Stylianos Somarakis, Heraklion, Greece

Submitted: September 21, 2017; Accepted: April 26, 2018
Proofs received from author(s): June 6, 2018